



## Modelling SOL flow pattern spreading in the edge plasma

L. Isoardi<sup>a</sup>, G. Ciraolo<sup>a,\*</sup>, G. Chiavassa<sup>a</sup>, P. Haldenwang<sup>a</sup>, E. Serre<sup>a</sup>, Ph. Ghendrih<sup>b</sup>, Y. Sarazin<sup>b</sup>, F. Schwander<sup>b</sup>, X. Garbet<sup>b</sup>, P. Tamain<sup>c</sup>

<sup>a</sup>M2P2 CNRS/Aix-Marseille Université, Technopole de Château Gombert, F-13451 Marseille, France

<sup>b</sup>IRFM,CEA-Cadarache, F-13108 St. Paul-lez-Durance Cedex, France

<sup>c</sup>EURATOM/UKAEA Fusion Association Culham Science Centre, Abingdon, Oxon OX14 3DB, UK

### A B S T R A C T

The transition region between closed and open magnetic flux surfaces plays a crucial role for tokamak performances. Appropriate understanding of the edge region remains a major challenge owing to several open issues as momentum transport, turbulence overshoot or neutral penetration. We consider here a transport model system to investigate the propagation of parallel momentum from the SOL into the core plasma and vice-versa. The numerical results show that for small values of the radial diffusion coefficient, the density profile decays exponentially from the core to the SOL as predicted by 1D analytical solution. A spreading of the parallel momentum from the SOL to the core is observed, with the presence of non-zero velocities also in the regions far from the SOL. The effect of an imposed rotation of the core plasma is investigated as well as the dynamics of an overdensity imposed in the core plasma.

© 2009 Elsevier B.V. All rights reserved.

### 1. Introduction

A better knowledge of the transport and turbulence phenomena occurring in the plasma edge of a tokamak is of great importance for increasing the quality of the confinement. It is now recognized that plasma rotation is a key element to estimate the confinement performance of future devices such as ITER [1]. Indeed, rotation will play a role on MHD activity as well as turbulent transport. For the latter, the transition region between closed and open magnetic flux surfaces plays a crucial role since an edge transport barrier can develop spontaneously in its vicinity [2]. This leads to the so-called H-mode regime that is the reference scenario for ITER. Appropriate understanding of the edge region remains a major challenge owing to several open issues as momentum transport, turbulence overshoot or neutral penetration. In this paper, the transition from the periodic (closed magnetic flux surfaces) to the non periodic region (open magnetic flux surfaces) in the parallel direction as well as the flow region around the limiter are considered. A second-order finite difference approximation associated with flux limiter scheme has been implemented in order to deal with sharp discontinuities of the solution in these regions. The spreading of SOL flow patterns into the edge plasma has been investigated. The physical and numerical modelling will be firstly presented. Then, numerical results will be analyzed according to the control parameters and boundary conditions.

### 2. Physical and numerical modelling

The minimal system to investigate the propagation of parallel momentum from the SOL into the core plasma involves two fields, the ion density  $n_i$  and the parallel particle flux  $\Gamma_{\parallel} = n_i v_{\parallel}$ . The ion and electron temperatures  $T_i$  and  $T_e$  are taken constant and due to the quasineutrality hypothesis, we have  $n_i = n_e = n$ . The conservation equations of both density and momentum in the parallel direction are treated in two dimensions (2D), namely the parallel  $s$  and the radial  $r$  coordinates, as follows:

$$\begin{cases} \partial_t n + \partial_s \Gamma_{\parallel} - \partial_r (D \partial_r n) = 0 \\ \partial_t \Gamma_{\parallel} + \partial_s (\Gamma_{\parallel}^2 / n) + c_s^2 \partial_s n - \partial_r (v \partial_r \Gamma_{\parallel}) = 0. \end{cases} \quad (1)$$

Here,  $c_s^2 = (T_e + T_i) / m_i$  is the sound speed (assumed constant), and  $D$  and  $v$  are the constant dissipative and viscous coefficients, respectively. The equations are derived from the classical conservation equations for compressible flows, where  $\Pi = \Gamma_{\parallel}^2 / n + c_s^2 n$  would be the total pressure (kinetic + thermodynamic). A dissipative term is added in the density equation to take into account the effect of turbulence fluctuations.

The geometric configuration (Fig. 1) mimics the transition region from the core (periodic boundary conditions) to the Scrape Off Layer (SOL) where the presence of the limiter causes the periodicity loss.

Boundary conditions have been imposed as shown in Fig. 1. Radially, a constant density gradient is assumed entering from the core with a zero parallel velocity. On the wall side, radial absorption conditions for density and parallel momentum are

\* Corresponding author.

E-mail address: [Guido.Ciraolo@L3M.univ-mrs.fr](mailto:Guido.Ciraolo@L3M.univ-mrs.fr) (G. Ciraolo).

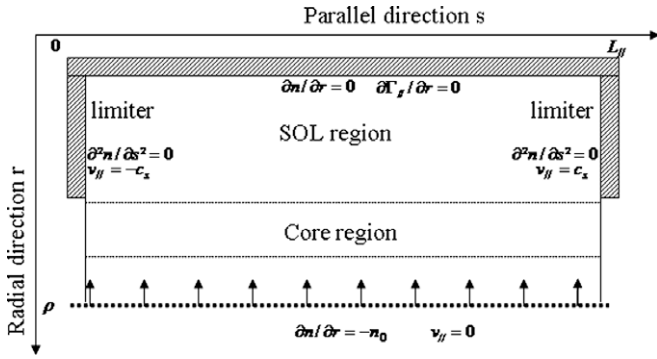


**Fig. 1.** 2D geometrical domain determined by the parallel direction  $s$  and the radial direction  $r$ . The domain includes the transition from the core to the SOL region up to the wall. The limiter is taken into account through the boundary conditions, imposing the plasma parallel velocity equals to plus or minus the acoustic velocity on the two opposite sides of the limiter, and the parallel gradient of plasma density equals to a constant. In the core region, periodic parallel boundary conditions are imposed. Radially, a constant density gradient is assumed as boundary condition on the core region. On the wall side, radial absorption conditions for density and parallel momentum are imposed.

imposed, i.e.  $\partial n/\partial r = 0$ ,  $\partial \Gamma/\partial r = 0$ . In the parallel direction  $s$ , the periodicity is assumed in the core region while in the SOL a constant velocity equal to  $\pm c_s$  is imposed on the two opposite sides of the limiter, as prescribed by the Bohm criterion [3]. Along the limiter, we have imposed  $\partial^2 n/\partial s^2 = 0$ , that is the parallel density flux is kept constant.

The dynamics is governed by the convection in the parallel direction and by diffusion in the radial direction, with different scales associated with these two phenomena. Eqs. (1) are normalized using the radial length  $\rho$  of the domain for the radial direction and the connection length of the magnetic field between two lim-

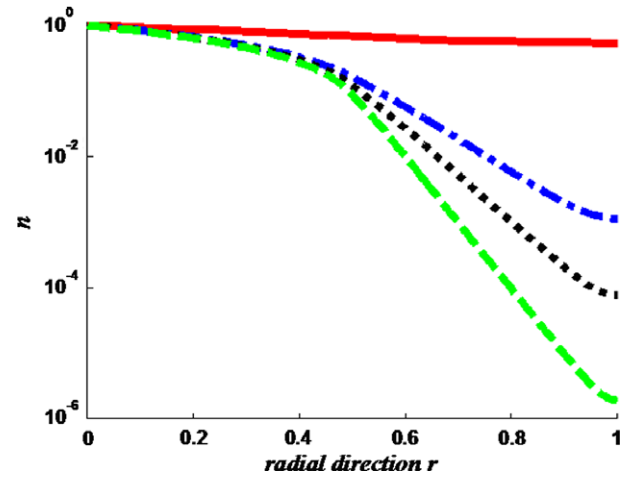


**Fig. 3.** Normalized radial profiles of density averaged in the parallel direction at  $Sc = 1$ . The SOL region corresponds to a radial coordinate from  $r = 0.5$  to  $r = 1$ . The four radial profiles are obtained for  $\tau = 0.5$  (red and solid line),  $\tau = 10^{-2}$  (blue and dash-dot line),  $\tau = 5 \times 10^{-3}$  (black dot line),  $\tau = 2.5 \times 10^{-3}$  (green and dash line). (For interpretation of the references to colour in this figure legend, the reader is referred to the web version of this article.)

its  $L_{||}$  for the parallel direction. The acoustic velocity  $c_s$  is the reference scale for the velocity. The time scale  $\tau_{||} = L_{||}/c_s$  is related to the parallel dynamics. The density is normalized by a constant and a-priori arbitrary density  $n_0$ . Finally, the parallel momentum scale is given by the product  $n_0 c_s$ . Then Eqs. (1) become for  $N$  and  $\Gamma$  the normalized density and parallel momentum:

$$\begin{cases} \partial_t N + \partial_s \Gamma - \tau (\partial_r^2 N) = 0 \\ \partial_t \Gamma + \partial_s (\Gamma^2/N) + \partial_s N - (\tau Sc) (\partial_r^2 \Gamma) = 0, \end{cases} \quad (2)$$

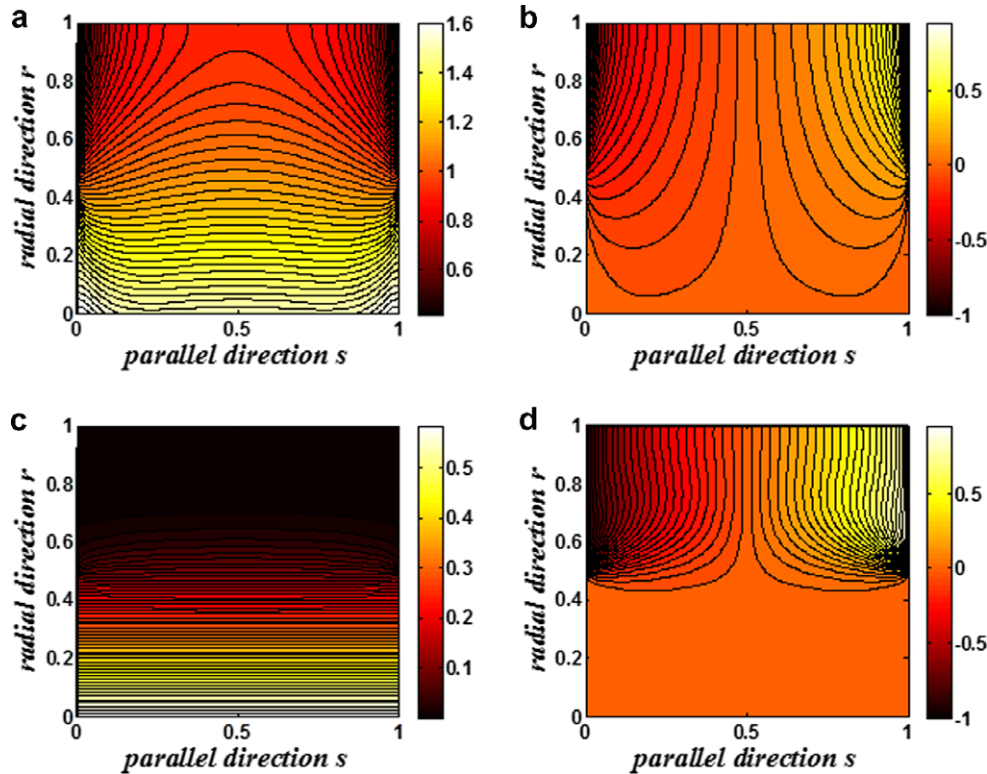


**Fig. 2.** Contours plot of density (a, c) and velocity (b, d) at the equilibrium at  $Sc = 1$ . The radial extension of the core region is between  $r = 0$  and  $r = 0.5$ . The SOL, with the limiter imposed on the two sides of the domain, is defined between  $r = 0.5$  and  $r = 1$ . The two top panels (a, b) where strong connection between the core and SOL is observed, are obtained for  $\tau = 0.5$ . The two bottom panels (c, d) where the two regions are much less connected are obtained for  $\tau = 10^{-2}$ .

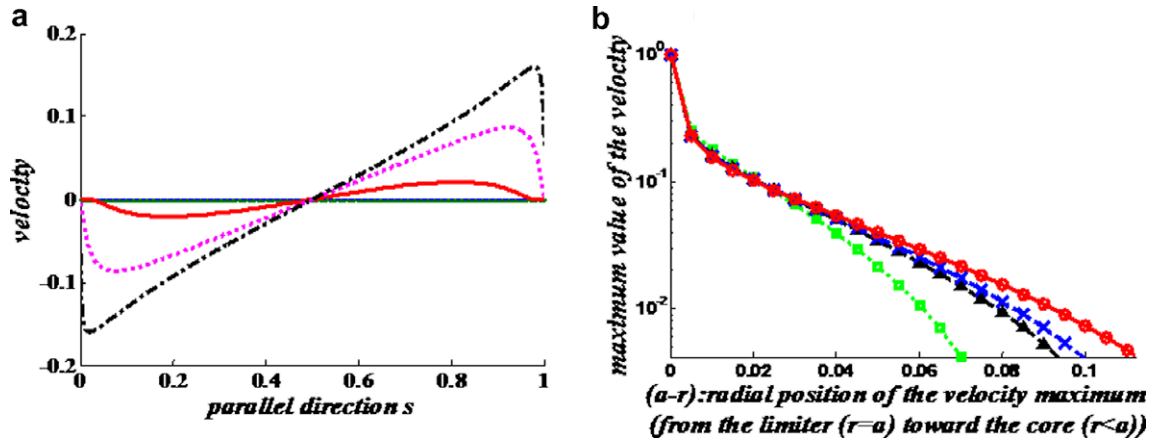


**Fig. 4.** (a) Parallel profiles of velocity at  $\tau = 10^{-2}$  and  $Sc = 1$  at different radii within the core, for  $r = 0$  (blue and solid line),  $r = 0.2$  (green and dot line),  $r = 0.44$  (red and solid line),  $r = 0.48$  (pink and dot line),  $r = 0.49$  (black and dash dot line). (b) Velocity maxima as a function of their radial position which is plotted from the limiter toward the core. The profiles are obtained for different values of the Schmidt number and for  $\tau = 10^{-2}$  kept fixed. The four profiles are for  $Sc = 0.1$  (green squares and dot line),  $Sc = 0.7$  (black up triangles and dash line),  $Sc = 1$  (blue crosses and dash dot line),  $Sc = 2$  (red circles and solid line). (For interpretation of the references to colour in this figure legend, the reader is referred to the web version of this article.)

for  $(r, s) \in [0, 1] \times [0, 1]$ . Dimensionless control parameters of the system are  $\tau = (DL_{||}/c_s \rho^2)$  and  $Sc = (v/D)$ .  $Sc$  is the Schmidt number and  $\tau$  the ratio of two times characterizing the parallel and radial dynamics. By analogy with fluid mechanics  $\tau$  can be written as the ratio  $A/Pe$ ,  $Pe$  being the Péclet number equal to  $\rho c_s/D$ , and  $A$  the aspect ratio of the cavity defined by  $A = L_{||}/\rho$ .

The Eqs. (2) are numerically solved using a second-order finite difference scheme. Approximation of advection terms is based on a TVD flux limiter scheme [4–5] to take into account shocks or sharp transitions in the parallel direction without introducing spu-

rious numerical oscillations. Radial diffusive terms are discretized implicitly for numerical stability reasons.

### 3. Transient and equilibrium flow patterns

The results show that there exist two transport regimes at the equilibrium in which the core and the SOL are connected (Fig. 2). These regimes are mainly controlled by  $\tau$  and remain qualitatively independent of the  $Sc$  number (radial diffusion of the parallel

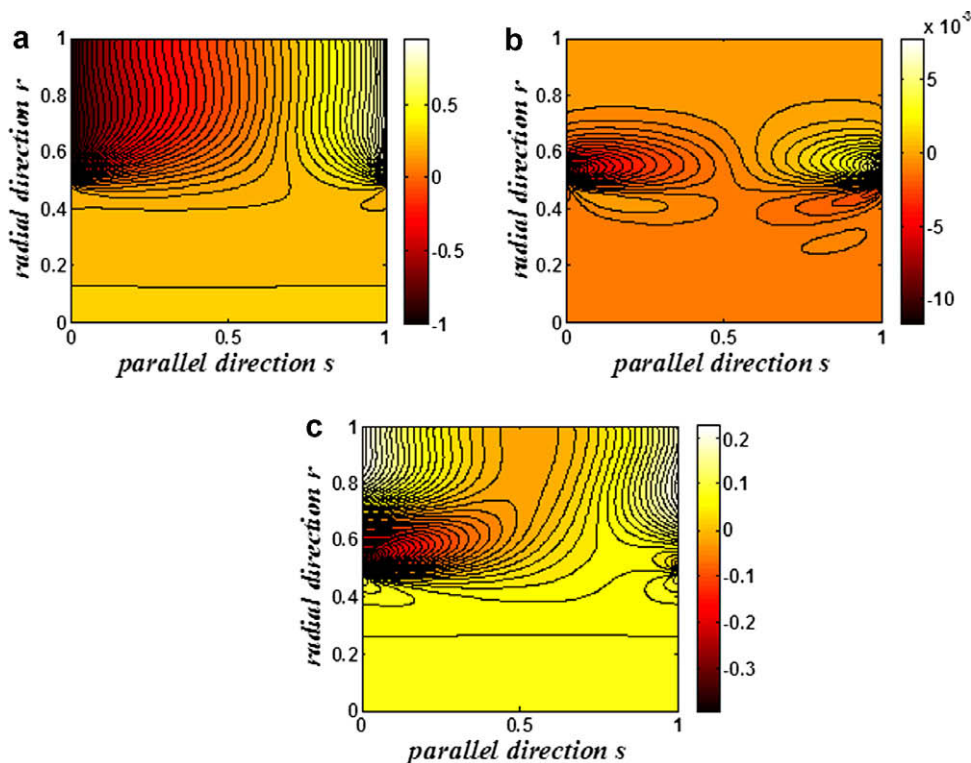


**Fig. 5.** (a) Contour plot of iso-velocity at  $\tau = 0.01$  and  $Sc = 1$ , with a mean parallel velocity  $V_{0||} = 0.3c_s$  imposed in the core side. (b) Contour plot for the difference between two density fields, one obtained with a mean parallel velocity imposed in the core side  $V_{0||} = 0.3c_s$  and the other one obtained with  $V_{0||} = 0$ . (c) Contour plot of the ratio  $(\Pi(V_{0||} = 0.3c_s) - \Pi(V_{0||} = 0))/\Pi(V_{0||} = 0)$  where  $\Pi = I^2/N + N$  is the pressure field.  $\Pi(V_{0||} = 0.3c_s)$  is obtained in the case of a mean parallel velocity  $V_{0||} = 0.3c_s$  imposed in the core side and  $\Pi(V_{0||} = 0)$  is obtained for  $V_{0||} = 0$ .

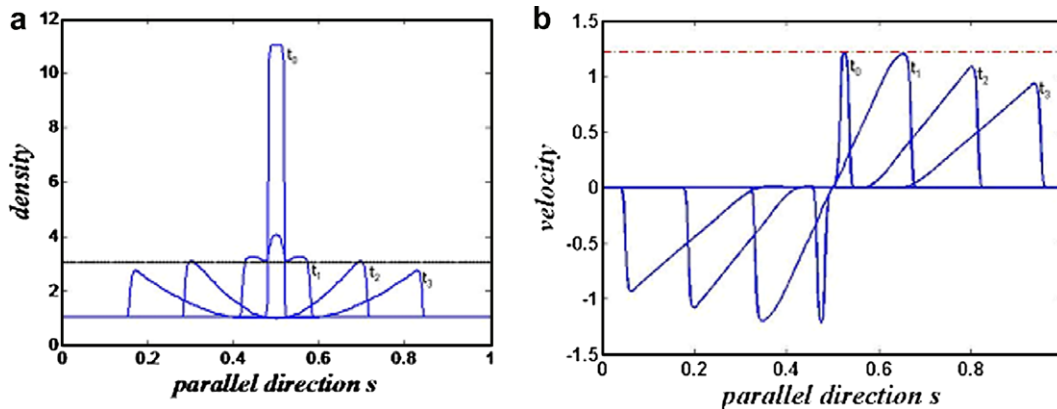


**Fig. 6.** Temporal evolution of parallel profiles of density (a) and velocity (b) of the shock wave at fixed radial position in the core at  $\tau = 0.01$  and  $Sc = 1$  with an increment  $\alpha = 10$ . The analytical solution for the velocity of the shock wave, represented by the dotted line, is computed using the value  $N^*$  of the density front at the beginning of the numerical simulation. A very good agreement is found with the numerical solutions at  $t_0$  and  $t_1$ . For  $t_3$  and  $t_4$  the analytical solution is not represented, but one can observe that the density front decreases and so its velocity, as expected from the theory.

momentum). For  $\tau$  of order one, the core and the SOL are strongly connected. Density injected from the core spread out into the SOL and reaches the wall and the limiter. Due to the Bohm conditions at the limiter, the speed strongly increases in the parallel direction to reach Mach number  $M = \pm 1$  on the two sides of the limiter. For small values of  $\tau$ , that is parallel dynamics which dominates on the radial one, only a small amount of density reaches the far SOL. The plasma is directly convected in the parallel direction but at a much lower speed than in the SOL. The solutions show that a limit  $\tau \approx 10^{-2}$  exists from which the solutions become qualitatively independent of  $\tau$  as illustrated by the averaged radial profiles of density in Fig. 3. The averaged density profile in the radial direction shows that the density exponentially decays between the core and the SOL. This behaviour is in agreement with an analytical density profile obtained at the equilibrium by averaging the density equations in the parallel direction [3]. On the contrary, at large  $\tau$ , the density remains almost constant between the core and the SOL. Thus the physical situation which corresponds to tokamak plasmas and that we will consider from now on is for the limit  $\tau \approx 10^{-2}$ .

The parallel momentum can nevertheless propagate from the SOL to the core by radial diffusion. This is illustrated by the parallel profiles of the velocity in the core region which show that non-zero velocities propagate far in the core (Fig. 4a). In Fig. 4b, we represent the maximum values of this parallel velocity in the core region for different  $Sc$  numbers. We observe the exponential behaviour of the velocity maximum from the last closed magnetic flux surface to the core region is slightly affected by the value of the  $Sc$  number.

In order to mimic plasma rotation into the core region observed in experiments, we introduce a non-zero parallel mean velocity  $V_{0||}$  in the core as a boundary condition. This core velocity breaks the symmetry of the flow pattern (Fig. 5a) shifting the parallel position of density maxima. This symmetry breaking is more evident for large  $\tau$  since the radial diffusion is larger. The maximum of dissymmetry is localized at the transition region between the last closed magnetic lines and the first open ones as shown in Fig. 5b for the density field. Numerically, we obtained that for  $V_{0||} \in [0, 0.5]c_s$ , this difference  $\Delta n$  increases linearly with  $V_{0||}$  as expected from a theoretical point of view.

Finally, we have studied the effect of a density perturbation introduced in the core region and superimposed on the initial condition at the first time step. Neglecting the radial terms in the Eq.

(2), one obtains a 1D non-linear Riemann problem [6] which admits an analytical solution. The flux  $\Gamma^*$  of the shock wave is determined by the equation  $\Gamma^* = N^* \log(\alpha N^*)$ , depending on the density  $N^*$  of the shock wave and on the initial density increment  $\alpha$ . We have compared the parallel velocity of the shock wave  $\Gamma^*/N^*$  obtained from the numerical simulations with the one expected from the analytical computation. The observed behaviour is in agreement with the analytical solution. The density peak splits into two symmetric peaks propagating in opposite directions (Fig. 6a) with supersonic (parallel) velocities (Fig. 6b). The agreement between analytical and numerical results validates the numerical modelling of the parallel dynamics.

#### 4. Concluding remarks

Numerical solutions of a 2D minimal transport model have been obtained for the edge plasma within the transition region between the core and the SOL. Numerical tools have been developed to treat accurately the transition region from closed magnetic surfaces to open magnetic surfaces, with the loss of periodicity due to the presence of a limiter in the SOL. The results show that the flow pattern is mainly governed by the density diffusion and indicate very sharp variations as well as spreading effects. At low diffusivity, spreading of parallel momentum into the core is observed around the limiter involving non-zero velocities far from the limiter in the radial direction. The 2D model considering temperature distribution is already in progress as well as a 3D version taking into account the dynamics in the poloidal direction. Such features are important to understand the edge/SOL interplay and model 3D effects including Kelvin Helmholtz instabilities that may be expected due to the strong shear on parallel velocity [7].

#### References

- [1] T. Tala et al., Plasma Phys. Control. Fus. 49 (2007) B291.
- [2] R.J. Groebner, Phys. Fluids B5 (1993) 2343.
- [3] P.C. Stangeby, The Plasma Boundary of Magnetic Fusion Devices, IOP, 2000.
- [4] C. Hirsch, Numerical Computation of Internal and External Flows, Wiley, 1990.
- [5] P.L. Roe, Annu. Rev. Fluid Mech. 18 (1986).
- [6] R.J. Leveque, Finite Volume Methods for Hyperbolic Problems, Cambridge Texts in Applied Mathematics, 2002.
- [7] X. Garbet et al., Phys. Plasmas 6 (1999) 3955.